J Mater Sci: Mater Med (2007) 18:405–413
DOI 10.1007/s10856-006-0706-5

# Is surface chemical composition important for orthopaedic implant materials?

**D. O. Meredith · M. O. Riehle · A. S. G. Curtis · R. G. Richards**

Received: 15 June 2006 / Accepted: 27 October 2006


**Abstract** Ti-6Al-7Nb (NS) in its 'standard' implant form has been previously shown to be detrimental to fibroblast growth and colonisation on its surface. Specific aspects of the NS topography have been implicated, however, the contribution of its unique surface chemistry to the cell behaviour was unknown. By evaporating either gold or titanium on the surface of standard NS, two different model surface chemistries could be studied with the same characteristic standard NS topography. Two other 'standard' orthopaedic topographies, that of stainless steel (SS) and of 'commercially pure' titanium (TS) were also treated in a similar manner. All materials elicited behaviour similar to their uncoated counterparts. For coated SS and TS, cell proliferation was observed, cells were well spread and displayed mature focal adhesion sites, and associated cytoskeletal components. For coated NS, cell proliferation was compromised, cells remained rounded, filopodia attached and seemed to probe the surface, especially the $\beta$-phase particles, and both the focal adhesion sites and the microtubule network were disrupted by the presence of these particles. These results confirmed, that in the instance of NS, the topography was the primary cause for the observed stunted cell growth. For biomaterials studies, the standardisation of surface chemistry used here is a valuable tool in allowing vastly different materials and surface finishes to be compared solely on the basis of their topography.

D. O. Meredith (✉) · R. G. Richards
AO Research Institute, AO Foundation, Clavadelerstrasse, CH-7270 Davos, Switzerland
e-mail: d.meredith@bio.gla.ac.uk

D. O. Meredith · M. O. Riehle · A. S. G. Curtis
Centre for Cell Engineering, Institute of Biomedical and Life Sciences, Joseph Black Building, University of Glasgow, Glasgow G12 8QQ, United Kingdom

## 1 Introduction

Ti-6Al-7Nb is a titanium alloy primarily utilised in orthopaedic implants such as intramedullary nails and bone screws [1–3]. While widely used in bone contact applications it has recently been introduced in some plate/screw application where it has contact with a more biologically complex environment of hard as well as soft tissue. We have previously studied soft tissue reactivity using an *in vitro* human fibroblastic cell model and found that 'standard' Ti-6Al-7Nb (NS) was detrimental to fibroblast spreading and growth, while a smooth electropolished (e.p) Ti-6Al-7Nb counterpart presented no problems in that fibroblasts grew to confluency [4].

The surface chemistry of Ti-6Al-7Nb is a heterogeneous mix of titanium, aluminium and niobium oxides found at the surface in relation to the underlying $\alpha$ and $\beta$ phase composition of the bulk alloy [5, 6]. For the acid etched 'standard' finish, denoted in this study as NS, the concentration of $Nb_2O_5$ on the surface has been quoted as being generally higher than on e.p surfaces, thus e.p cannot be used as a topographical control for NS [6]. Acid etching, usually a mix of nitric and hydrofluoric acid, effectively dissolves the outer layer of the material cleaning and roughening the surface. The authors have previously presented evidence that the topography is a contributing factor in affecting numerous cellular functions [7]. However, can these observations be replicated in the absence of NS's unique surface chemistry or is this factor also integral to its performance? The cellular effect of Ti-6Al-7Nb component oxides have been studied previously using a fabricated topography mimicking the spatial distribution of the various oxides, based upon the relation of the bulk $\alpha + \beta$ phases [8, 9]. In this instance, it was observed that cells were sensitive to the varying oxide chemistries.

Kasemo and Lausmaa noted that the biochemical interaction of a metal surface with biological material was limited to

**Table 1** Summary of materials used and processes employed in the course of their manufacture

| Material | Denoting symbol | Raw material | Band grinding (grit[a]) | Vibratory grinding (ceramic tumbling) | Ball blasted | Pickled (acid etching) | Electropolished | Anodised | Gamma sterilised |
|---|---|---|---|---|---|---|---|---|---|
| Ti-6Al-7Ni | NS[b] | Bar | 220 & 320 | √ | INOX | √ | – | Gold (57V) | √ |
| cp. Titanium | TS[b] | Sheet | 320 | √ | INOX[c] | √ | – | Gold colour (55V) | √ |
| Stainless steel | SS[b] | Sheet | 320 | – | – | – | √(Mathys AG) | - | √ |

[a]Ceramic grit particle size.
[b]Material in 'standard form'.
[c]INOX stainless steel balls.

the top layer with a maximum thickness of 1 nm [10]. As the naturally forming titanium oxide layer is between 2–5 nm, and in the case of industrial anodisation up to 50 nm [5], the cells will never interact with the underlying bulk metal [10, 11]. Coating titanium onto various materials is a commonly utilised method to create surfaces in order to mimic implants. This overlying homogenous metal chemistry has been exploited in numerous biomaterial studies using epoxy-resin of metal surfaces [12–14] and fabricated microtopographies amongst others [15–17], and it effectively masks the underlying surface chemistry from any biological interaction.

The hypothesis put to the test here is that the surface topography of NS was the sole cause of the detrimental cellular reactions observed. To test this hypothesis the surface chemistry of the NS was masked by coating the surface with either 50 nm gold or 50 nm titanium. Gold is considered bioinert and biocompatible [17] and titanium is biocompatible as it forms an inert titanium-oxide upon contact with air [18, 19]. By using two separate metals, two different surface chemistry models could be studied in relation to the characteristic NS topography. Two other 'standard' orthopaedic topographies of elecropoloished stainless steel (SS) and 'commercially pure' titanium (TS) (roughened similar to NS) were also treated in a similar manner and served as controls. The orthopaedic 'standard' finish of these materials varies considerably with TS roughened and anodised in a similar manner to NS, while SS is electropolished. These two materials were previously demonstrated to present no difficulty for fibroblast adherence and growth [4], however the question could be raised: is this effect entirely dependent on their 'standard' topographies?

## 2 Materials and methods

### 2.1 Material preparations

All materials, Ti-6Al-7Nb (NS) (ISO 5832/11), Stainless Steels (SS) (ISO 5832/1) and 'commercially pure' titanium (TS) (ISO 5832/2) were sourced from Mathys Medical AG (Bettlach, CH) stock. Discs of 12.7 mm in diameter (1–2 mm thick) were prepared from all materials. A summary of important steps utilized in material preparation and consequent characterisation is included in Table 1. The samples were evaporated with either 50 nm of gold or 50 nm of titanium and were consequently referred to as either e.g. NG or NT. Evaporation was performed using an e-beam evaporator (MEB450, Plassys, UK) utilising pure gold or titanium plate source material for evaporation. The coating was carried out in a Grade 2 Nanofabrication Laboratory (James Watt Nanofabrication Centre, University of Glasgow) therefore contaminants were kept to a minimum and the samples sealed until final use in a Category 2 laminar flow cabinet. For cell work the samples were ethanol (70%) sterilised after coating following rinses in sterile reverse osmosis $H_2O$.

### 2.2 Material characterisation

The surface topography of each sample was quantitatively measured with a noncontact "white-light" FRT MicroProf 200 Profilometer (Fries Research & Technology, Germany). Roughness average (Ra—arithmetic mean of the roughness height) was measured from a $2 \times 2$ mm analysis area scan at a point density of 500 points/mm. Prior to roughness calculations a linear regression to eliminate surface inclinations was performed on each profile with the Lc (cutoff) set to 0.4 mm. For each surface six separate areas were scanned on two samples of each surface. The morphology of the disc surfaces was examined using a Hitachi S4100 field emission scanning electron microscope (FESEM) fitted with an Autrata yttrium aluminium garnet (YAG) backscattered electron (BSE) scintillator type detector. The images were taken in both the secondary electron mode (SE) and BSE, with an accelerating voltage of 5 kV, an emission current of 50 $\mu$A, an aperture of 100 $\mu$m (apt1), working distance of 12 mm, and a positive tilt of 15°. For X-ray photoelectron spectroscopy (XPS) all spectra were recorded on a Kratos Axis Nova (Kratos Analytical, UK) using monochromated AlK$\alpha$ radiation (1486.69 eV) produced at an anode power of 225 W (15 kV, 15 mA), an electron take-off angle of 90°

relative to the surface plane, and an electron analyzer pass energy of 80 eV. During analysis the base pressure remained below 10–8 torr. For quantification, survey scans with a step width of 0.5 eV were performed on two spots of 300 × 700 $\mu m^2$ per sample. Two points per sample type were assessed and the data was evaluated with CasaXPS 2.3.10 (CasaXPS Ltd, UK) using relative sensitivity factors supplied with the instrument.

### 2.3 Cell seeding, fixation and SEM

Infinity telomerase immortalized primary human fibroblasts (hTERT-BJ1, Clonetech Laboratories, Inc., USA) were seeded onto the 12.7-mm sample discs at 5000 cells per 0.5 mL of medium [71% Dulbecco's Modified Eagles Medium (DMEM) (Sigma, UK), 17.5% Medium 199 (Sigma, UK), 9% fetal calf serum (FCS) (Life Technologies, UK), 1.6% 200 mm l glutamine (Life Technologies, UK), and 0.9% 100 mm sodium pyruvate (Life Technologies, UK)]. The cells were incubated at 37°C with a 5% $CO_2$ atmosphere for 24 h, 5 and 10 days with the culture media changed every 2.5 days.

The cells (12-mm discs) were fixed in 4% paraformaldehyde in 0.1M PIPES (Piperazine-NN -bis-2-ethane sulphonic acid, Fluka, CH), pH 7.4 for 5 min. The cells were postfixed in 0.5% osmium tetroxide (Oxkem, UK) in 0.1 M PIPES, pH 6.8 for 1 h. The cells were dehydrated through an ethanol series (50, 60, 70, 80, 90, 96, and 100%) followed by a Fluorisol/Ethanol series (25, 50, 75, and 100%) (Fluorisol—1,1,2 trichloro,1,2,2, trifluoro ethane). The samples were critical point dried with a critical point drier (Structure Probe Inc. UK), mounted on aluminium stubs and sputter coated with a 10-nm layer of gold/palladium (80 Au/20 Pd) using a Baltec MED 020 sputter coater (Baltec, FL). Samples were imaged using an Hitachi S-4100 FESEM operated as noted above.

### 2.4 Vinclin, Tubulin, Actin and DNA staining and fluorescence microscopy

Cells were seeded on the samples (5000 per 0.5 ml) and cultured for 48 h. The samples were fixed in 4% formaldehyde/PBS (phosphate buffer solution) (with 2% sucrose) for 15 min, incubated for 5 min with the permeabilising buffer (10.3 g sucrose, 0.292 g NaCl, 0.06 g $MgCl_2$, 0.476 g HEPES buffer, 0.5 ml Triton X, in 100 ml water, pH 7.2) and blocked using 1%BSA/PBS (bovine serum albumin) for 5 min. Samples were incubated either 1:100 mouse monoclonal anti-Vinculin (clone hVin-1, Sigma) or 1:50 mouse anti-$\beta$-Tubulin (Sigma, Cat No. T4026) and 1:50 Phalloidin (Rhodamine conjugated, Molecular Probes, UK) suspended in 1%BSA/PBS for 1 h (37°C). After washing with 0.5% Tween 20/PBS (3 × 2 min) samples were incubated with 1:50 horse biotinylated anti-Mouse (Vector Laboratories, UK) for 1 h (37°C). Samples were rinsed with 0.5% Tween 20/PBS (3 × 2 min) and incubated with 1:50 Fluorescein Streptavidin (Vector Laboratories) for 30 min (4°C). After a final wash with 0.5% Tween 20/PBS (3 × 2 min) the samples were mounted with Vectashield with DAPI (4',6-diamidino-2-phenylindole) (Vector Laboratories).

Samples were imaged using a Zeiss Axiovert 200 M inverted microscope fitted with an Evolution QEi Monochrome (MediaCybernetics, UK) camera. Fluorescent light was supplied by a HBO 100 mercury lamp (Zeiss, DE) and reflected light for imaging the metallic substrate supplied by a HAL 100 (12 V, 100 W, Zeiss) lamp. Samples were imaged with lens magnifications of ×20 and ×40 objectives, captured using Image-Pro Plus Version 5.1 (MediaCybernetics, UK) with a separate pass required for each filter and reflected light image. Pseudocoloured images were assembled using Photoshop 7.0 (Adobe, USA) in RGB mode. Reflected light images were superimposed with 50–60% opacity.

### 2.5 Cell counts and statistical analysis

Cells were seeded on the uncoated and coated sets of samples in triplicate for each sample type and for the three timepoints—24 h, 5 and 10 day. For the 5 and 10 day samples, the media was changed every 2.5 days. Cells were fixed, permeabilised, incubated with rhodamine conjugated phalloidin and mounted with DAPI. For each sample a minimum of 15 images at ×10 lens magnification (Zeiss Axioplan 2) taken randomly on the surface, totalling 45 images for each set. This was repeated for all sample types at all timepoints. Cell counts were conducted using ImageJ 1.33 m (1997–2006, National Institute of Health, http://rsb.info.nih.gov/ij/) to process the DAPI images by counting the nuclei. Statistical analysis was conducted for each original material type, e.g SS and coated counterparts, and also time intervals. The question posed was if there is any difference in cell numbers with regards to the surface coating and not between the original sample types. Due to the nature of cell seeding, variation on a single replicate was high, therefore the means of the three replicates per sample type were utilised for the analysis. For each sample batch a two-way analysis of variance (ANOVA) was conducted at $p < 0.01$ using Statlets© (1997, NWP Associates, Inc. http://espse.ed.psu.edu/statistics/statlets/statlets.htm) to examine for any significant differences.

## 3 Results

### 3.1 Surface chemistry masking

The effectiveness of the mask was assessed using SEM in BSE mode to determine the homogeneity of the coating and

**Table 2** Prolfilometry and XPS results for the original uncoated sample variants and gold or titanium coated variants

| | Surface coating (50 nm) | Denoting symbol | Ra | XPS |
|---|---|---|---|---|
| Ti-6Al-7Nb (NS) | Uncoated | NS | $0.77 \pm 0.076$ $\mu$m | Al: 2.5%, C: 24.5%, O: 51.7%, P: 2.6%, Ti: 16.6%, Nb: 0.3% |
| | Gold | NG | $0.83 \pm 0.018$ $\mu$m | Au: 51.8%, C: 35.6%, O: 12.6% |
| | Titanium | NT | $0.82 \pm 0.056$ $\mu$m | C: 22.2%, N: 0.7%, O: 52.7%, Ti: 24.4% |
| cp. Titanium (TS) | Uncoated | TS | $0.90 \pm 0.027$ $\mu$m | C: 25.7%, O: 52.6%, P: 3.1%, Ti: 16.7% |
| | Gold | TG | $0.88 \pm 0.017$ $\mu$m | Au: 58.5%, C: 34.9%, O: 6.6% |
| | Titanium | TT | $0.85 \pm 0.029$ $\mu$m | C: 25.6%, N: 1.2%, O: 51.7%, Ti: 21.6% |
| Stainless Steel (SS) | Uncoated | SS | $0.19 \pm 0.022$ | C: 29.5%, Cr: 9.1%, Fe: 3.3%, 2.6%, Na: 2.7%, O: 46.9%, P: 1.7%, Si: 3.1% |
| | Gold | SG | $0.17 \pm 0.022$ $\mu$m | Au: 37.4%, C: 38%, O: 24.6% |
| | Titanium | ST | $0.18 \pm 0.008$ $\mu$m | C: 23.7%, N: 0.9%, O: 52.3%, Ti: 23.2% |

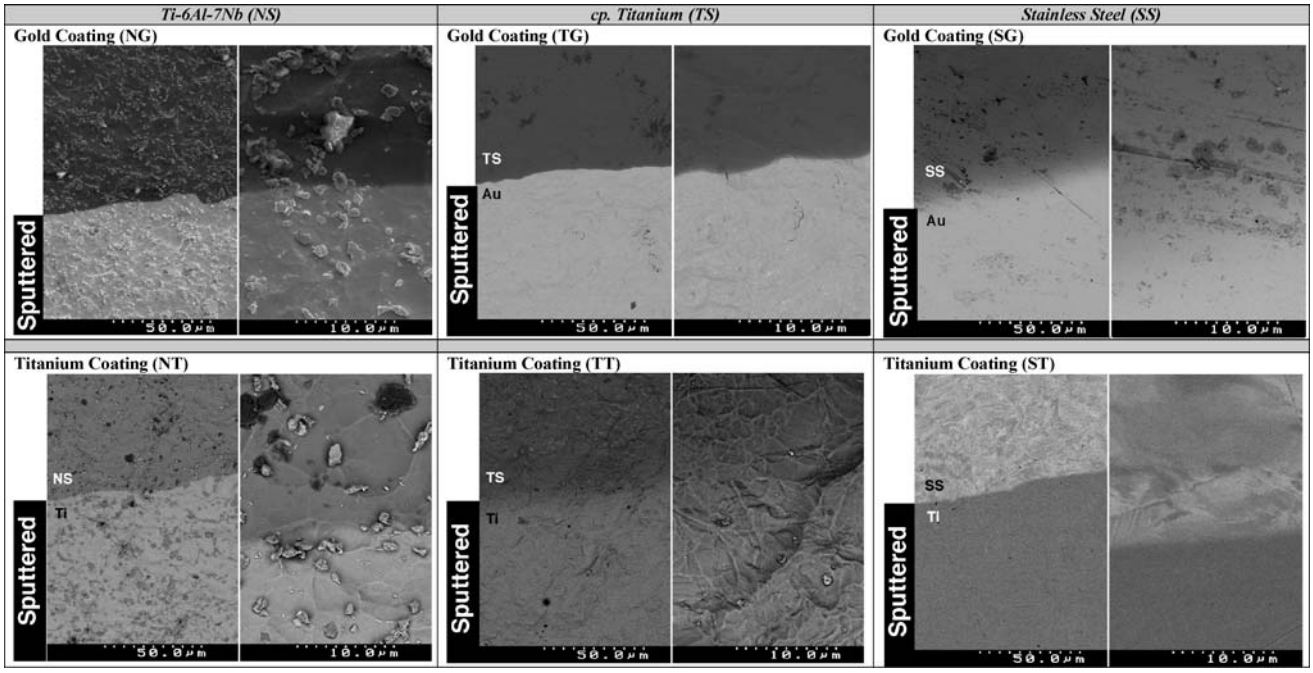


**Fig. 1** SEM of the gold and titanium coated variants of the 3 core sample types

ensure the maintenance of notable surface features with reference to their previously characterised uncoated counterparts [4]. Included in Fig. 1 are images taken at the border between uncoated and coated material for all sample types; these images clearly demonstrate the compositional difference, in the instance of SS and NS, between the chemical heterogeneity of the underlying original surface and the homogeneity of the coated surface. Profilometry was utilised to look for any modifications to the surfaces on a larger scale. For each surface type (e.g., SS) the measurements were similar, and furthermore, when compared with uncoated versions of the original materials, no differences were observed (Table 2). Analysis of the surface chemistry by means of XPS, confirmed that both the surface coatings were effective in masking the original, underlying surface chemistry. These measurements are summarised in Table 2.

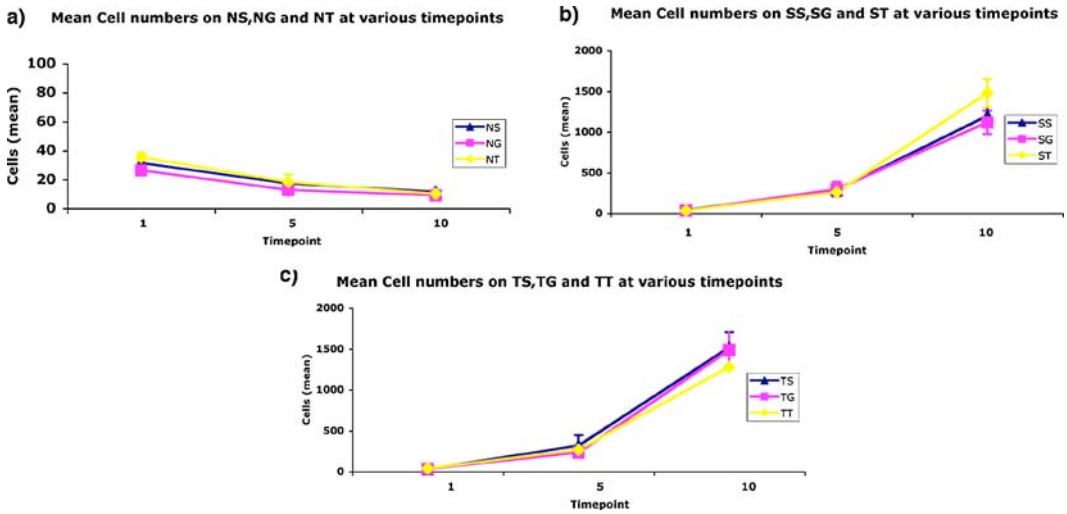


**Graph 1** Plot of mean cell counts ($n = 45$), for a 1418 $\mu$m × 1128 $\mu$m field of view, at the three timepoints, for each standard surface type and modified surfaces coated with either gold or titanium. Plot (a) is for NS, (b) SS, (c) TS. Note that the scale for NS is lower than the other plots to allow the smaller differences in numbers to be displayed. Cell growth was compromised on NS and its coated counterparts. Cell growth was observed on coated and uncoated SS and TS

### 3.2 Quantitative cell growth

With the exception of NS, NG and NT, all other materials supported cell growth to a confluent monolayer by 10 days. The cell counts confirmed that for each surface cell growth followed a similar trend, with or without masking of the surface chemistry (Graph 1). This was also analysed statistically, where the only statistical significance found between a set of coated and uncoated sample types e.g. SS, SG and ST, was between the three timepoints ($p < 0.01$). Cell numbers on NS, NG and NT were consistently low and statistically, a significant difference was only observed between the three timepoints ($p < 0.01$).

### 3.3 Cell morphology and intracellular labelling

High magnification SEM, and fluorescence imaging (48 h, vinculin, tubulin, actin and DNA) of cells on the coated samples was conducted to ensure that qualitatively there were no outstanding discrepancies in the features noted of cells found on the coated surfaces in comparison to the uncoated samples examined in previous studies [4, 7]. No differences were observed, which supported the analysis of cell growth observations for each set of surfaces. These qualitative features are summarised in Table 3 and selectively represented in the following figures (Figs. 2–4).

As stated previously, the main focus of the investigation was cell reactivity towards NS and its coated counterparts. Cell counts for the cells on the different chemistries were not statistically different, and at higher magnifications the cell morphology on both NG and NT was unspread or elongated with a ruffled membrane, similar to those cultured on uncoated NS at 24 hr (Fig. 2). For the majority of cells observed on NS, filopodia projected from points closer to the nucleus, and these attached on the surface primarily to the protruding topography of the $\beta$-phase particles (Fig. 2(a), (c), (e), (g)). For NG, it was apparent in both SE and more clearly in BSE that small patches of the coating had come away from the surface exposing the original underlying surface (Fig. 2(b) and (d)). The shape of the patches indicates that these were sites of loose $\beta$-phase particles that had been removed, however, the scattered nature of the areas would suggest that involvement of cells in the removal process was unlikely. It was more plausible that the particles had come off during the culturing or SEM preparation phases. An absence of filopodia interacting with these patches indicates that the cells did not perceive the areas of differing surface chemistry, which would suggest that the cells primarily interacted with the topography. Another plausible explanation for this lack of a reaction would be that these patches had only become exposed post-fixation (Fig. 2(d)). Due to the low atomic number contrast between the surface coat and the original surface on NT, it was difficult to observe any traces of $\beta$-phase particle removal in this instance (Fig. 2(f) and (g)).

Fluorescence labelling on coated NS demonstrated small punctuate focal adhesion sites avoiding the $\beta$-phase particles, restricted spreading and intermittent breaches in the microtubule network at the site of protruding particles. Examples of cells on NG are included in Fig. 3. Labelling of adhesion sites on coated SS demonstrated well spread cells with mature focal adhesion sites and associated actin cytoskeleton (SG example in Fig. 4(a)). Cells on coated TS were not as well spread as on the smoother surface of SS, and the focal adhesions

**Table 3** Summary table of the qualitative and quantitative observations for hTERT cells cultured of SS, TS and NS and their counterparts coated with either 50 nm gold or titanium. All qualitative observations are described apart from '√' which denotes that the surface did not affect the labelled structure. For quantitative measures; '+/+' indicates a high value and '−/−' a low value

| | | Cell morphology | | Intracellular staining | | |
|---|---|---|---|---|---|---|
| Sample type | Cell growth | Spreading | Filopodia | Cytoskel. | Microtubules | Focal adhesions |
| SS | +/+ | Spread cells | Minimal | √ | √ | 'Dash' |
| SG | +/+ | Spread cells | Minimal | √ | √ | 'Dash' |
| ST | +/+ | Spread cells | Minimal | √ | √ | 'Dash' |
| TS | +/+ | Visible spreading alignment to the topography | Highly prominent on cells at 24 hr and 5 days utilised to sense the topography | √ | √ | Smaller adhesions |
| TG | +/+ | Visible spreading alignment to the topography | Visible at 24 hr and 5 days | √ | √ | Smaller adhesions |
| TT | +/+ | Visible spreading alignment to the topography | Visible at 24 hr and 5 days | √ | √ | Smaller adhesions |
| NS | −/− | Elongated or unspread morphology | Interacting with the particulate topography at all timepoints | √ | Network punctuated with holes at the sites of protruding particulates | Smaller adhesions, visibly influenced by the topography |
| NG | −/− | Elongated or unspread morphology | Interacting with the particulate topography | √ | Holes at sites of of protruding particles | Smaller, influenced topography |
| NT | −/− | Elongated or unspread morphology | Interacting with the particulate topography | √ | Holes at sites of protruding particles | Samller influenced by topography |

were not as dense or large as those on the smoother surfaces (TG example in Fig. 4(b)). However, these observations are in line with those of cells on uncoated TS, and this did not affect downstream cell growth on the uncoated or coated surfaces [4, 7].

## 4 Discussion

Using profilometry, SEM and XPS, surface characterisation of the modified surfaces demonstrated that the coating technique and thickness had effectively masked the samples, including NS. SEM in BSE mode demonstrated this clearly; in most instances the atomic number contrast of the coating was sufficiently different from the underlying sample surface to reveal a homogenous mask of the surfaces and their features, with the exception of TT. Profilometry Ra calculations revealed no differences between coated and uncoated samples, thus the large-scale sample topography remained unchanged. SEM also demonstrated that at the smaller scale, the evaporating process generally did not introduce any new roughness. XPS demonstrated that the surface chemistry of the materials was now dependent on the coating type, rather than the original material composition. It is apparent that the evaporating method has successfully reproduced two different sets of standard topographies with homogenous surface chemistries. This enabled cellular reactions to the topography to be concluded minimising the involvement of the chemistry.

The coating of SS and TS with either gold or titanium elicited identical reactions to their uncoated counterparts both qualitatively and quantitatively. Cells on coated SS and TS were well spread, their intracellular structure was unaffected in displaying mature focal adhesion sites and associated actin cytoskeleton, a well conserved radiating microtubule structure, and cell growth to confluency at later timepoints observed on all surfaces. Cell behaviour on SS and TS indicated that the surface chemistry on these materials did not play a role in cell reactions and that both these topographies were favourable to cell colonisation.

Cell behaviour on NS agreed with that observed on the other coated materials, in that there were no significant variations in cell growth that were dependent on the surface coating. Generally, cells at all timepoints demonstrated an unspread or elongated morphology, the cell filopodia attached and probed the coated surface and particles, and both the focal adhesion sites and the microtubule network were disrupted by the presence of the particles. These results were in keeping with those observed previously for NS, and further strengthened the hypothesis that the specific microspiked topography found on NS (and coated counterparts) was the contributing factor in restricting cell spreading and adhesion, ultimately resulting in poor colonisation of the surface.

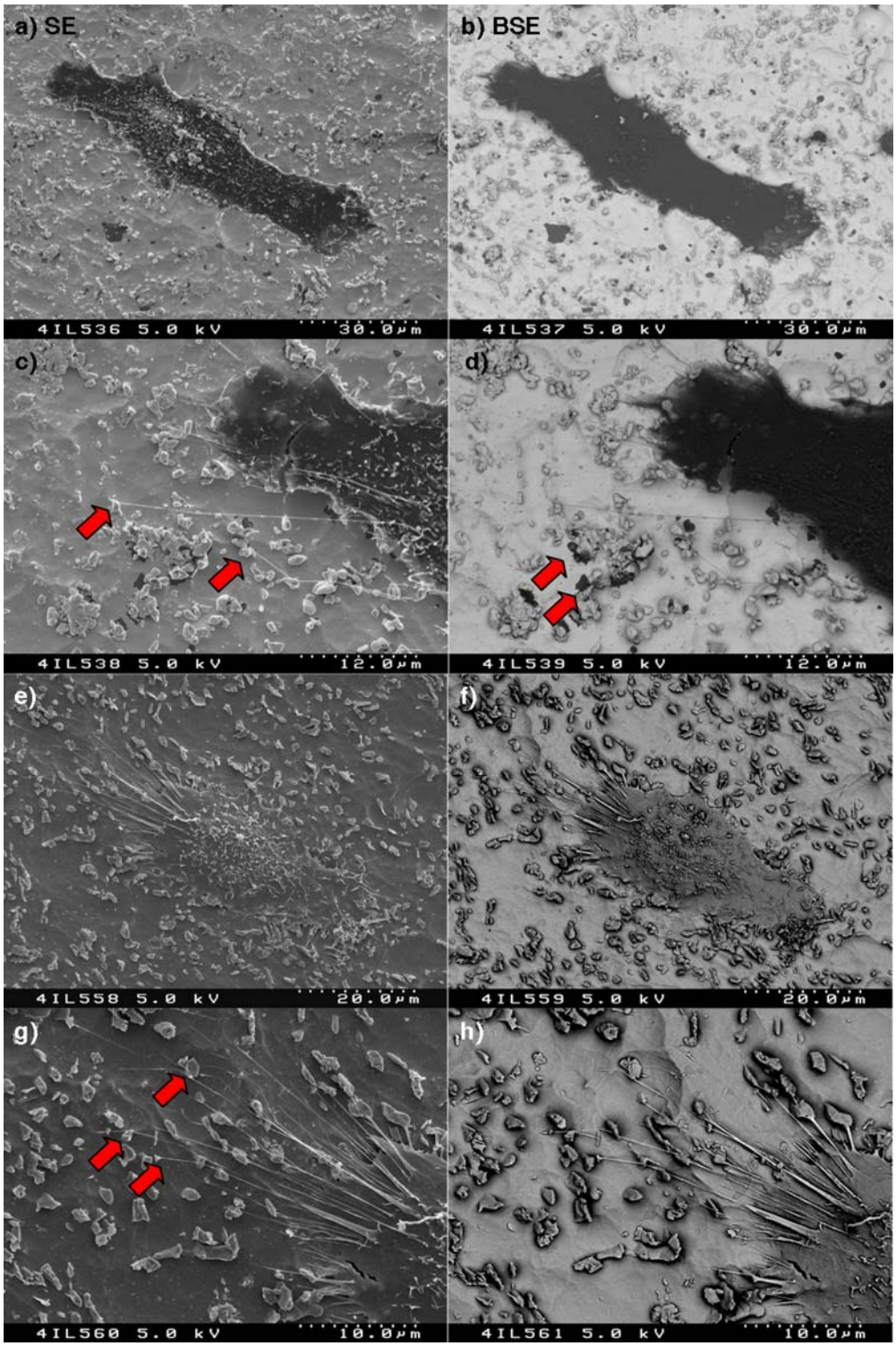


**Fig. 2** Cells cultured for 24 h on NG (a-d) and NT (e–h). Left column of images are SE (secondary electron) and right are BSE (backscattered electron) of the same cell, (a) SE mode image the cell morphology was generally unspread with a ruffled membrane and protruding filopodia (b) BSE demonstrated that small patches of the coating covering the surface area had come away from the surface. (c) Numerous filopodia extended from the cell body and attached to the protruding $\beta$-phase particles (red arrows). (d) The shape of the coating gaps would suggest that these were in fact site of loose $\beta$-phase particles that have been removed (red arrows). (e) On NT the cell remains unspread and demonstrates numerous filopodia extending from the cell body. (f) The lower atomic number contrast between the surface coat and the original surface made it difficult to see any traces of $\beta$-phase particle removal. (g) Filopodia attaching and bridging the titanium coated $\beta$-phase particles (red arrows). (h) High magnification BSE further demonstrates the elemental homogeneity of the surface

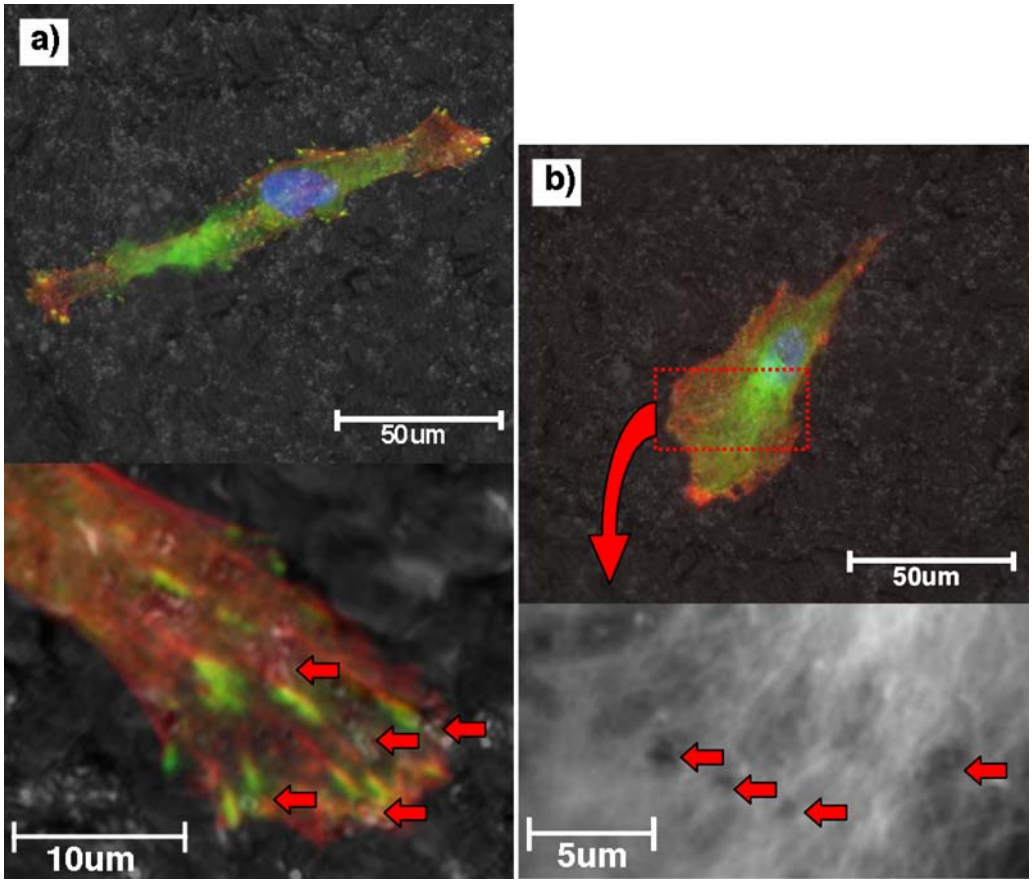


**Fig. 3** Cell cultured on NG for 48 h and (a) Triple labelled for Vinculin (green), Actin (red) and DNA (blue). Cells were generally elongated or unspread with small 'dot' like focal adhesion sites. These sites could be observed avoiding particles present on the surface (red arrows). (b) Tubulin (green), Actin (red) and DNA (blue). The microtubule network was present throughout the cell body, however it was punctuated with gaps corresponding to particles protruding from the surface (red arrows)

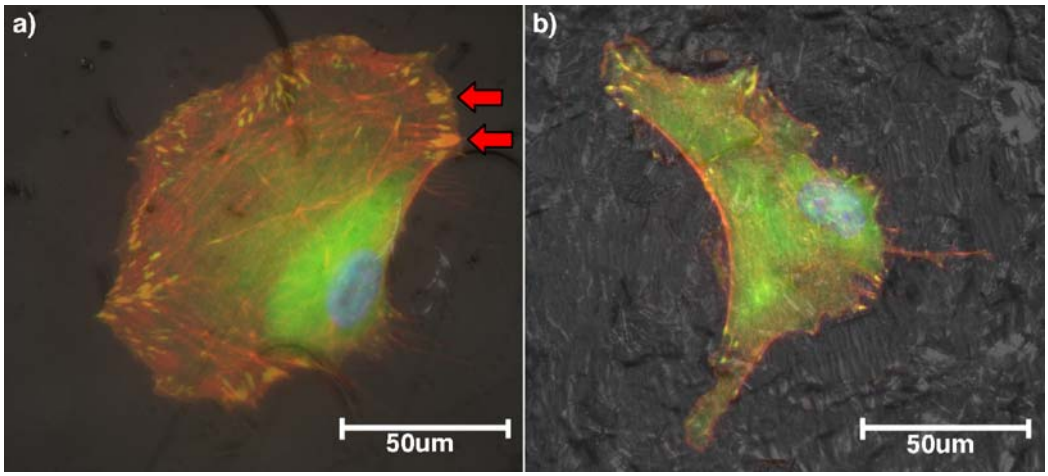


**Fig. 4** Cell cultured for 48 h and triple labelled for Vinculin (green), Actin (red) and DNA (blue) on (a) SG: Cells were generally very well spread with mature focal adhesion sites (red arrow) and associated actin cytoskeleton stretching between parallel cell peripheries. (b) TG: On the rougher surface cell were not as well spread and neither were the focal adhesions as dense or large as those on the smoother surface. The actin cytoskeleton demonstrated arching at the cell periphery indicative of spreading on a rough surface

It is highly probably that surface chemistry contributed no involvement in the poor growth and colonisation of NS.

The atomic number contrast of the gold-coated NS (NG) surface yielded an additional observation helping to clarify the cause of particle removal on NS. In an earlier study we hypothesised this particle removal was due to cell removal and endocytosis of loosened particles, however, this could not be confirmed (unpublished results) [4]. By examining high magnification SEM images of cells cultured on NG, holes in the coating could be observed surface-wide, and these holes were of similar dimensions to the $\beta$-phase particles. This surface-wide removal of particles could not be due only to cell interaction as previously suspected, it was more plausible that the immersion in culture media, and/or the cell fixation protocol could cause removal of the loosened particle. If the removal occurs at this point of time, this reinforces the observation that NS topography was the primary factor for cell behaviour as no reactivity to the exposed underlying surface chemistry was observed, but rather filopodia probed the coated particles. This phenomenon could not be seen by atomic number contrast on NT due to similarity of the coatings' atomic number contrast to that of the underlying surface.

Coating the standard materials with a uniform chemistry provided a practical model to investigate how surface chemistry and the various topographies interact in their effect on cells. There are other methodologies for the production of surface replicas, generally involving the production of a negative die or mould that can consequently be utilised to reproduce positive replicas [12–14]. These have been used with great success in the study of the effect of different roughness of titanium, and would be beneficial for the study of both SS and titanium—however, initial attempts with NS in its standard form have proven to be difficult as during the demoulding of the replica the resin also removed some of the looser $\beta$-phase particles from the surface. With regard to fibroblast surface interaction, the $\beta$-phase particles were identified in this study to be NS's most significant characteristic, and the absence of a portion of these particles, as would be the case with replica production, could influence any results obtained from using a replica. For biomaterials studies, the standardisation of surface chemistry is a valuable tool in allowing vastly different materials and surface finishes to be compared solely on the basis of their topography. Indeed, the factor of topography alone has been demonstrated in this study to be a very important element in ascertaining biomaterial cytocompatibility.

**Acknowledgments** Materials were supplied from the Robert Mathys Foundation, Bettlach, Switzerland, Grant No. P03E117/SLIPSURF with special thanks to Lukas Eschbach. The authors would also like to thank of Mary Robertson, Sara McFarlane and Chris Wilkinson at the Department of Electrical Engineering, University of Glasgow for coating the samples. We would also like to thank Christoph Sprecher from the AO Research Institute, Davos for his assistance.

## References

1. K. KRAMER, in "Materials for Medical Engineering: EUROMAT- Volume 2" (Wiley-VHC, Weinheim, New York, 2000) p. 9.
2. J. A. DISEGI, in "AO ASIF: Titanium—6% Aluminium—7% Niobium Implant Material" (AO Technical Commission, 1993) p. 1.
3. M. WINDLER, and R. KLABUNDE, in "Titanium in Medicine" (Springer, Berlin, 2001) p. 703.
4. D. O. MEREDITH, L. ESCHBACH, M. A. WOOD, M. RIEHLE, A. CURTIS and R.G. RICHARDS, *J. Biomed. Mater. Res. A.* **75A** (2005) 541.
5. J. A. DISEGI, in "Sixteenth Southern Biomedical Engineering Conference" (IEEE, 1997) p. 129.
6. C. SITTIG, M. TEXTOR, N. D. SPENCER, M. WEILAND and P. VALLOTTON, *J. Mater. Sci.: Mater. Med.* **10** (1999) 35.
7. D. O. MEREDITH, L. ESCHBACH, M. O. RIEHLE, A. S. G. CURTIS and R. G. RICHARDS, Submitted (2006).
8. C. A. SCOTCHFORD, M. BALL, M. WINKELMANN, J. VOROS, C. CSUCS, D. M. BRUNETTE, G. DANUSER and M. TEXTOR, *Biomaterials.* **24** (2003) 1147.
9. M. WINKELMANN, J. GOLD, R. HAUERT, B. KASEMO, N. D. SPENCER, D. M. BRUNETTE and M. TEXTOR, *Biomaterials.* **24** (2003) 1133.
10. B. KASEMO and J. LAUSMAA, *Int. J. Oral. Maxillofac. Implants*. **3** (1988) 247.
11. B. KASEMO, *J. Prosthetic Dent.* **49** (1983) 832.
12. M. WIELAND, B. CHEHROUDI, M. TEXTOR and D. M. BRUNETTE, *J. Biomed. Mater. Res.* **60** (2002) 434.
13. M. WIELAND, M. TEXTOR, B. CHEHROUDI and D. M. BRUNETTE, *Biomaterials.* **26** (2005) 1119.
14. M. SCHULER, G. R. OWEN, D. W. HAMILTON, M. DE WILD, M. TEXTOR, D. M. BRUNETTE and S. G. TOSATTI, *Biomaterials.* **27** (2006) 4003.
15. D. M. BRUNETTE, in "Titanium in Medicine" (Springer, Berlin, 2001) p. 485.
16. R. JAIN and A. VON RECUM, *J. Invest. Surg.* **16** (2003) 263.
17. J. TAN and W. M. SALTZMAN, *Biomaterials.* **23** (2002) 3215.
18. K. P. DEE, D. A. PUELO and R. BIZIOS, in "An Introduction To Tissue-Biomaterials Interactions" (John Wiley & Sons Inc., 2002).
19. B. D. RATNER, in "Titanium in Medicine" (Springer, Berlin, 2001) p. 1.